Electronic Supplementary Information

Highly Effective Organic Light-Emitting Diodes Containing Thermally Activated Delayed Fluorescence Emitters with Horizontal Molecular Orientation

Chan Hee Lee[a], Shin Hyung Choi[a], Sung Joon Oh[a], Jun Hyeon Lee[a], Jae Won Shim[b], Chihaya Adachi [c,d] and Sae Youn Lee [a,]*

[a]*Department of Energy and Materials Engineering, Dongguk University, Seoul, 04620, Republic of Korea*

[b]*School of Electrical Engineering, Korea University, Seoul, 02841, South Korea*

[c]*Center for Organic Photonics and Electronics Research (OPERA), Kyushu University, 744 Motooka, Nishi, Fukuoka, 819-0395, Japan*

[d]*Department of Chemistry and Biochemistry, Kyushu University, 744 Motooka, Nishi-ku, Fukuoka 819-0395, Japan*

[*]Corresponding author.

E-mail address: saeyounlee@dongguk.edu

Contents:

A. Instrument

NMR spectra were recorded on an Avance III 500 spectrometer (Bruker). Chemical shifts of ^{1}H NMR signals were quoted to tetramethylsilane (δ = 0.00) as an internal standards. Matrix-assisted laser desorption ionization time-of-flight (MALDI-TOF) mass spectra were collected on a Autoflex III spectrometer (Bruker Daltonics) using dithranol as the matrix. Elemental analyses were carried out with a Yanaco MT-5 CHN corder. The UV/vis absorption and PL spectra of organic films were measured with a UV-2550 (Shimadzu) and a FluoroMax-4 spectrofluorometer (Horiba Scientific), respectively. The photoluminescence quantum efficiency (Φ_{PL}) was measured using an absolute PL quantum yield measurement system (Hamamatsu Photonics C9920-02, PMA-11). Luminescence intensity and lifetime of organic films were measured with a Streak camera (Hamamatsu Photonics C4334). The organic films were excited by an N_2 gas laser (λ = 337 nm, pulse width = 500 ps, repetition rate 20 Hz) under a vacuum of $< 4\times10^{-1}$ Pa. Samples were cooled down at 5 K with a cryostat (Iwatani Industrial Gases). The density-functional theory (DFT) computations were performed on the Gaussian 09 program package, using the B3LYP functional with the 6-31G(d,p) basis set. Angular-dependent PL spectra of 6 wt% emitter-doped PPT films (15 nm thick) were measured to determine the molecular orientation. The sample consisted of a glass substrate was attached to a fused silica half-cylinder prism with a refractive index-matching liquid and an excitation CW laser at the wavelength of 375 nm with a power less than 20 mW was irradiated onto the film. Through a cutoff filter, a polarizer, and a collimating lens, PL intensity in a transverse magnetic mode was detected by a monochromator (PMA-11, Hamamatsu Photonics). The PL intensities were acquired in each out-of-plane angle from 0° (vertical to the substrate surface) to 90° (horizontal to the substrate surface), with a step of 1° (C14234-11; Hamamatsu Photonics). The obtained PL intensity angle-dependent patterns were analyzed using a commercial software package (Setfos 3.4, Fluxim).

B. NMR spectra

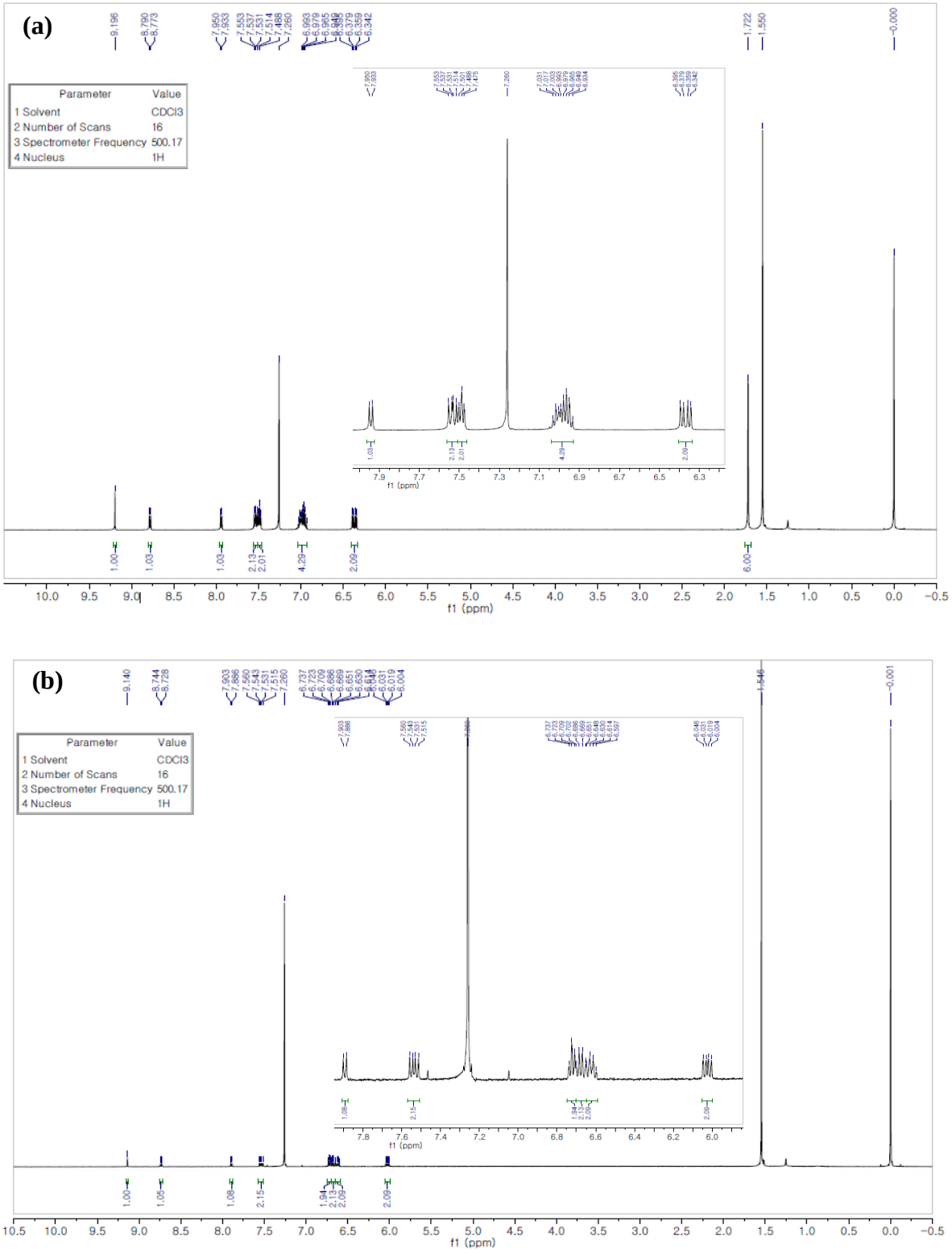

Fig. S1. ^{1}H NMR of (a) **AcPYM** and (b) **PxPYM**.

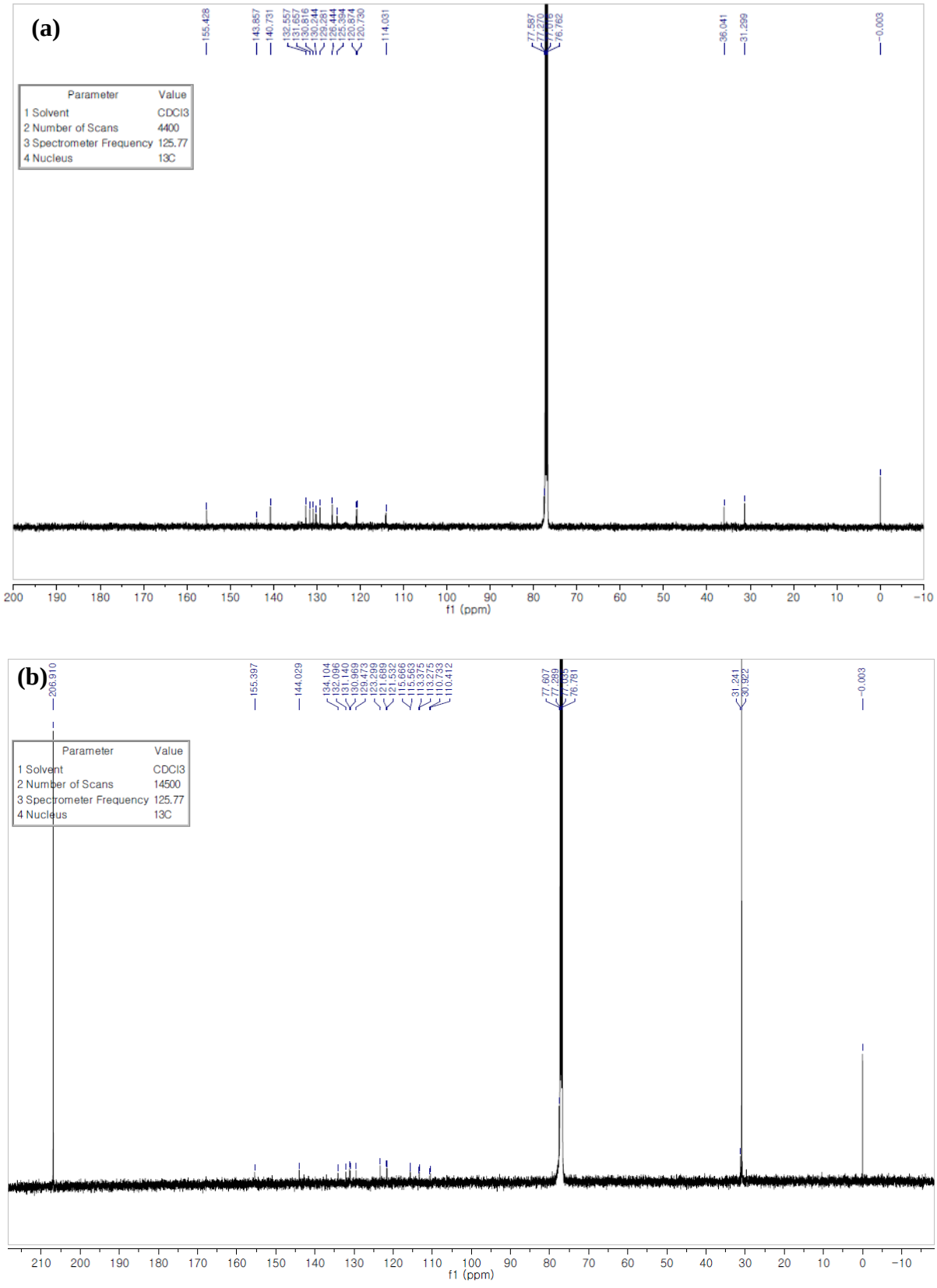

Fig. S2. ^{13}C NMR of (a) **AcPYM** and (b) **PxPYM**.

C. TD-DFT calculations data

Table S1. Triplet and singlet excitation energies (vertical transition), oscillator strength (*f*), and transition configurations of **AcPYM** and **PxPYM** calculated by TD-DFT at the B3LYP/6-31G(d,p).

Emitter	State	*E* [eV]	*f*	Main configuration [a)]		ΔE_{ST} [eV]
AcPYM	S_1	2.420	0.0000	H→L	0.6991	0.006
	S_2	2.632	0.0000	H-1→L	0.6957	
				H-1→L+3	0.1215	
	T_1	2.414	0.0000	H→L	0.6986	
	T_2	2.626	0.0000	H-1→L	0.6947	
				H-1→L+3	0.1252	
PxPYM	S_1	2.102	0.0002	H→L	0.6994	0.006
	S_2	2.311	0.0005	H−1→L	0.6963	
				H−1→L+3	0.1169	
	T_1	2.096	0.0000	H→L	0.6988	
	T_2	2.306	0.0000	H−1→L	0.6954	
				H−1→L+3	0.1213	

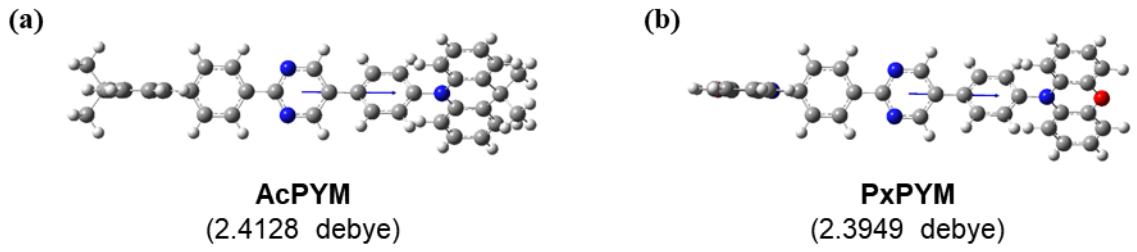

Fig. S3. The optimized molecular structure and transition dipole moments of (a) **AcYPM** and (b) **PxPYM**.

D. Thermal and photophysical properties

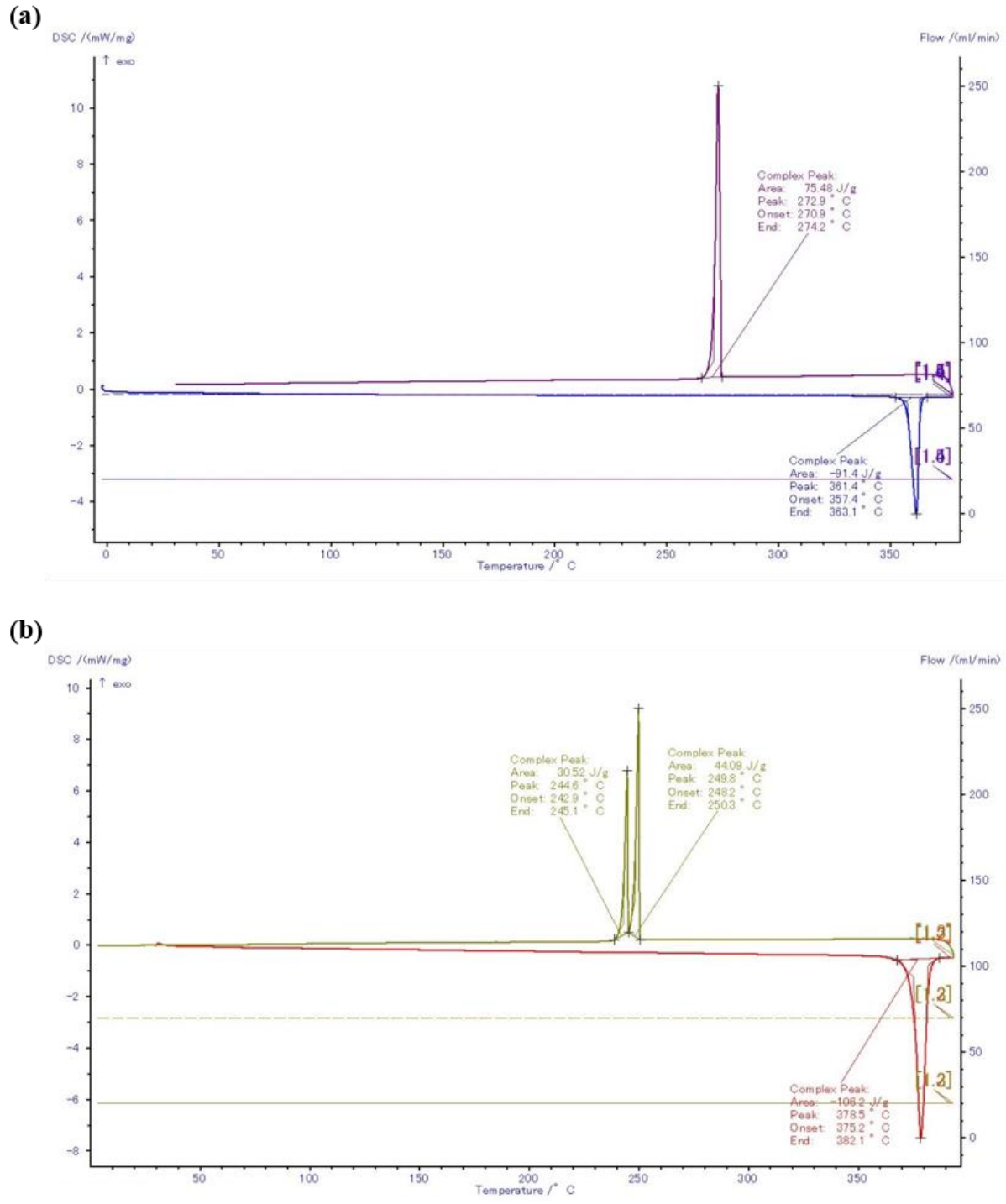

Fig. S4. DSC profiles of (a) **AcPYM** and (b) **PxPYM**.

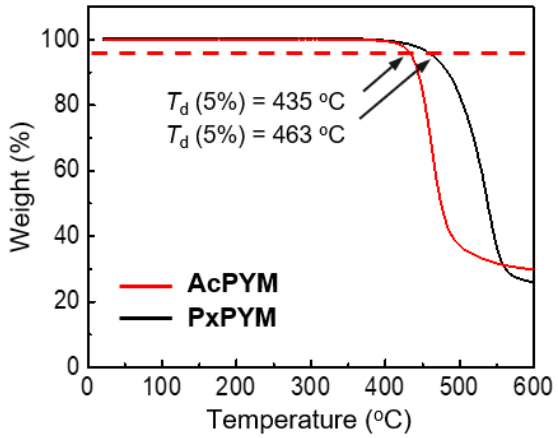

Fig. S5. TGA profiles of **AcPYM** (red) and **PxPYM** (black).

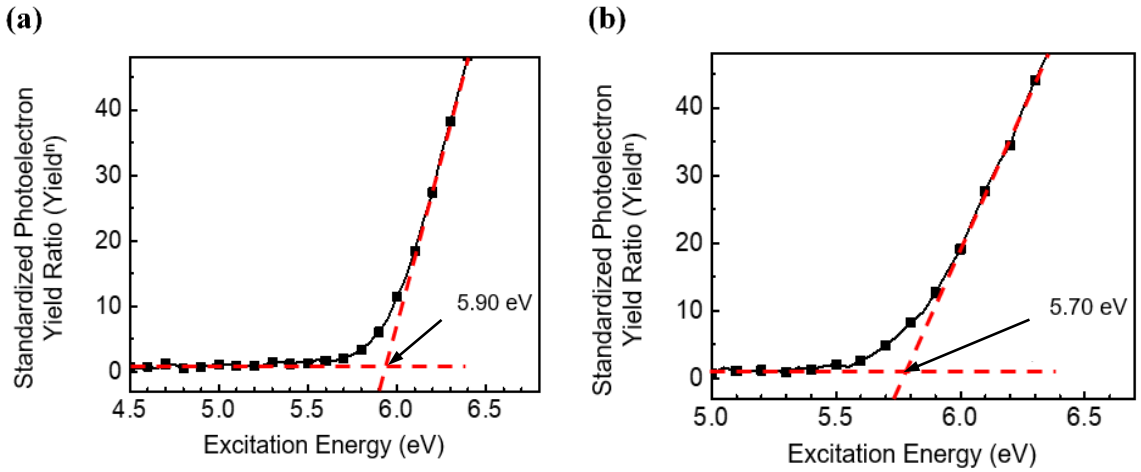

Fig. S6. Photoelectron yield spectra of (a) **AcPYM** and (b) **PxPYM**.

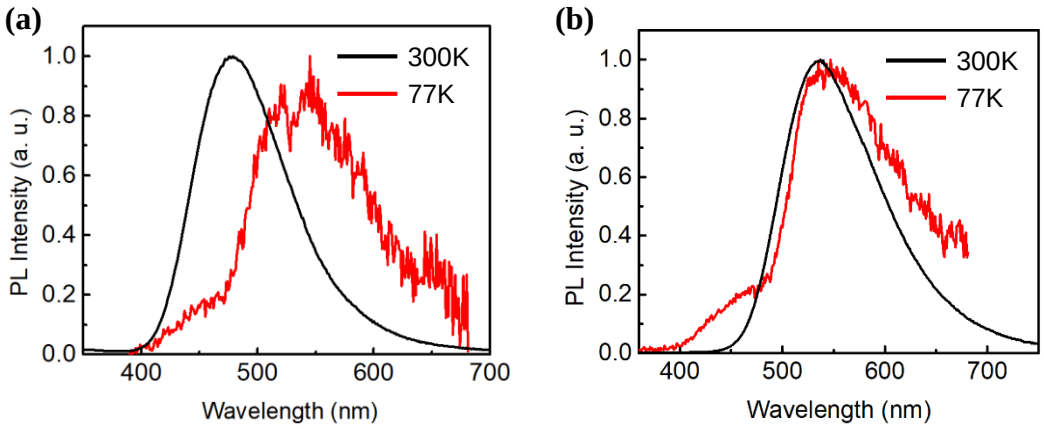

Fig. S7. PL and spectra of prompt luorescence at 300 K (black) and phosphorescence at 77 K (red) for (a) **AcPYM** and (b) **PxPYM**.

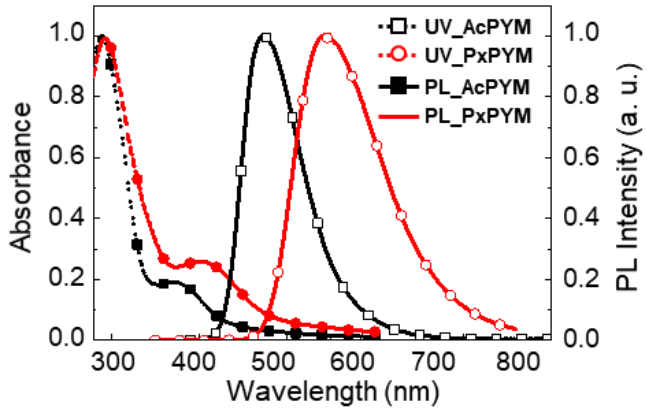

Fig. S8. UV-Vis and PL spectra of (a) **AcPYM** and (b) **PxPYM** neat film.

Table S2. Photophysical properties of **AcPYM** and **PxPYM** in solution[a)] and neat film.

Emitter	λ_{abs} [nm]		λ_{PL} [nm]		Φ_{PL} [%]			
	solution	neat	solution	neat	solution		neat	
					air	N_2	air	N_2
AcPYM	375	374	477	474	31.0	44.9	33.0	34.9
PxPYM	394	403	532	540	32.5	64.6	50.5	54.0

[a)] in toluene, 10^{-4} M

E. Determination of rate constants

Table S3. Rate constants and quantum efficiencies of **AcPYM** and **PxPYM**[a)].

Emitter	k_r^S [s^{-1}][b)]	k_d [s^{-1}][c)]	k_{ISC} [s^{-1}][d)]	k_{RISC} [s^{-1}][e)]	k_{nr}^T [s^{-1}][f)]	Φ_{ISC} [%][g)]	Φ_{RISC} [%][h)]
AcPYM	2.2×10^7	2.1×10^3	3.0×10^7	9.0×10^2	1.7×10^3	89.3	11.9
PxPYM	2.4×10^7	3.5×10^3	3.5×10^7	5.3×10^3	1.3×10^3	63.3	58.1

[a)]Measured using 6 wt.% **AcPYM**:PPT and **PxPYM**:PPT co-deposited films. [b)]Radiative decay rate constant of S_1 state, $k_r^S = \Phi_p/\tau_p$. [c)]Radiative decay rate constant of delayed fluorescence, $k_d = 1/\tau_d$. [d)]Radiative decay rate constant of ISC, $k_{ISC} = k_p - k_r^S - k_{nr}^S$, $k_{nr}^S \approx 0$. [e)]Radiative decay rate constant of RISC, $k_{RISC} = (k_p \times k_d \times \Phi_d)/(k_{ISC} \times \Phi_p)$. [f)]Non-radiative decay rate constant of T_1 state, $k_{nr}^T = k_d - (\Phi_p \times k_{RISC})$. [g)]Efficiency of ISC, $\Phi_{ISC} = 1 - \Phi_p$. [h)]Efficiency of RISC, $\Phi_{RISC} = \Phi_d/\Phi_{ISC}$.